IOP Publishing Environ. Res. Lett. 10 (2015) 084024 doi:10.1088/1748-9326/10/8/084024

Environmental Research Letters

OPEN ACCESS

RECEIVED
15 April 2015

ACCEPTED FOR PUBLICATION
30 July 2015

PUBLISHED
25 August 2015

LETTER

Is anthropogenic sea level fingerprint already detectable in the Pacific Ocean?

H Palanisamy[1], **B Meyssignac**[1], **A Cazenave**[1,2] **and T Delcroix**[1]

[1] LEGOS-UMR5566, Toulouse, France
[2] ISSI, Bern, Switzerland

E-mail: hindumathi.palanisamy@legos.obs-mip.fr

Keywords: tropical Pacific Ocean, internal climate mode, anthropogenic sea level fingerprint, altimetry based sea level, CMIP5 dynamic sea level

Abstract

Sea level rates up to three times the global mean rate are being observed in the western tropical Pacific since 1993 by satellite altimetry. From recently published studies, it is not yet clear whether the sea level spatial trend patterns of the Pacific Ocean observed by satellite altimetry are mostly due to internal climate variability or if some anthropogenic fingerprint is already detectable. A number of recent studies have shown that the removal of the signal corresponding to the Pacific Decadal Oscillation (PDO)/Interdecadal Pacific Oscillation (IPO) from the observed altimetry sea level data over 1993–2010/2012 results in some significant residual trend pattern in the western tropical Pacific. It has thus been suggested that the PDO/IPO-related internal climate variability alone cannot account for all of the observed trend patterns in the western tropical Pacific and that the residual signal could be the fingerprint of the anthropogenic forcing. In this study, we investigate if there is any other internal climate variability signal still present in the residual trend pattern after the removal of IPO contribution from the altimetry-based sea level over 1993–2013. We show that subtraction of the IPO contribution to sea level trends through the method of linear regression does not totally remove the internal variability, leaving significant signal related to the non-linear response of sea level to El Niño Southern Oscillation (ENSO). In addition, by making use of 21 CMIP5 coupled climate models, we study the contribution of external forcing to the Pacific Ocean regional sea level variability over 1993–2013, and show that according to climate models, externally forced and thereby the anthropogenic sea level fingerprint on regional sea level trends in the tropical Pacific is still too small to be observable by satellite altimetry.

1. Introduction

Sea level change is one of the most concerning consequences of climate change. Since the early 1990s, sea level is rising at a rate of 3.2 ± 0.4 mm yr^{-1} (e.g. Church *et al* 2013, Ablain *et al* 2015). Though a recent study, Watson *et al* (2015), has shown that the sea level rate over the altimetry period might be lower than previously estimated, all studies agree that sea level will continue to rise in the future because of expected continuing ocean warming and land-ice melt (Church *et al* 2013). Sea level rise is far from being uniform and exhibits significant spatial variations regionally mainly related to non-uniform thermal expansion and salinity variations of the ocean (e.g., Cazenave and Cozannet 2014, *Stammer et al* 2013, Church *et al* 2013, Levitus *et al* 2012, Fukumori and Wang 2013). For example, since 1993, rates up to three times the global mean rise are observed in regions like the western tropical Pacific (e.g. Merrifield and Maltrud 2011), north Atlantic around Greenland and southern Austral Ocean while other regions like the eastern tropical Pacific face lower rates of sea level rise (Bromirski *et al* 2011, Thompson *et al* 2014). Regional steric sea level changes in different ocean basins are attributed to differential heating and freshening of various ocean layers and associated physical processes such as air-sea interaction, lateral and vertical mixing or advective

processes (Yin *et al* 2010) with ocean circulation changes playing a major role (Stammer *et al* 2013). In addition other phenomena such as net ocean mass changes from melting land-ice as well as gravitational and solid earth responses due to Glacial Isostatic Adjustment (GIA) also contribute to regional sea level variability (e.g. Milne *et al* 2009, Stammer *et al* 2013), however their effects are small over the two recent decades. In the tropical Pacific, Merrifield, 2011, Merrifield and Maltrud, 2011 and Palanisamy *et al* 2015 showed that the high sea level trends in this region during the altimetry era are essentially due to the heat redistribution in the ocean related to the deepening of the thermocline in response to intensified trade winds.

The different contributors to sea level and thus sea level itself respond to unforced internal variability and forced variability of the climate system. While the unforced internal variability is spontaneously generated by the climate system in the absence of changes in the climate forcing, the forced variability is in response to external climate forcing which includes anthropogenic signal as well as natural forcing such as volcanic eruptions or solar variability. While at the global scale (i.e. in terms of global mean sea level), detecting and separating the internally generated climate modes from externally forced signals in sea level has been feasible (Marcos and Amores 2014, Slangen *et al* 2014), performing similar studies on regional sea level is highly challenging. This is because the internal climate variability introduces strong changes in regional sea level on time scales from years to decades (Richter and Marzeion 2014) and makes the signal to noise ratio very unfavorable in the detection of the forced response above the unforced internal variability. For example, the regional sea level changes in the tropical Pacific Ocean are governed by natural climates modes such as El Niño Southern Oscillation (ENSO) and Pacific Decadal Oscillation (PDO)/Interdecadal Pacific Oscillation (IPO) at interannual and decadal time scales, respectively (e.g. Stammer *et al* (2013), Zhang and Church (2012), Han *et al* (2013) Hamlington *et al* (2014a) and references therein). The internal sea level variability related to such climate modes of the order of $\pm$10–20 cm can therefore mask sea level changes due to externally forced signals.

Recently, making use of climate models from the fifth phase of the Coupled Model Intercomparison Project (CMIP5), studies (Lyu *et al* 2014, Jordà 2014, Richter and Marzeion 2014, Bilbao *et al* 2015) have determined the time of emergence, that is, the time when the anthropogenic climate change signal exceeds and emerges from the natural climate variability at a regional scale. Lyu *et al* (2014) find that relative to the 1986–2005 reference period, under RCP4.5 and RCP8.5 scenarios, the externally forced trend would be detectable in both steric and dynamic sea levels by the early to mid-2040s in 50% of the ocean. Similarly Richter and Marzeion (2014) also find that the externally forced signal is detectable in the early 2030s relative to 1990 in 50% of the ocean. These regions include the South Atlantic Ocean, Arctic Ocean, eastern Pacific Ocean and most parts of the Indian Ocean. Furthermore Jordà (2014) has shown that on average, it would require a minimum time period of 40 years to identify the externally forced signal at the regional scale. However in regions with strong decadal and interannual sea level variability, the emergence time increases up to 60–80 years. These results are also in agreement to that of Richter and Marzeion (2014) and Lyu *et al* (2014). This shows that the presence of strong internal variability can mask the long-term forced trend for several decades.

One method for determining the externally forced signal in sea level at the regional scale will be to remove the internal variability signal from the observed sea level at the region of interest and relate any residual signal to an externally forced signal. This has been the subject of two recent studies, Hamlington *et al* (2014a) and Palanisamy *et al* (2015) in the tropical Pacific. Since PDO/IPO is the main natural climate mode in this region (Han *et al* 2013, Hamlington *et al* 2014a), Hamlington *et al* (2014a) removed its contribution to sea level from the altimetry-based sea level signal over 1993–2012 and showed a residual trend pattern in the tropical Pacific that, in general, cannot be due to PDO. Using a modelling approach, this study also showed that the residual pattern after having removed the influence of PDO could be linked to anthropogenic warming of the tropical Indian Ocean (see Han *et al* (2013) for details). By removing the contribution of IPO from the mechanism that contributes to sea level changes in this region (i.e. the thermocline attributed steric sea level), Palanisamy *et al* (2015) showed a similar residual trend pattern in the tropical Pacific, but concluded that this residual pattern may alternately reflect the signature of other natural climate modes or some non-linear PDO signatures that were not properly removed in the process.

In this study we investigate this issue further. We perform a detailed analysis on the residual sea level trend pattern after having removed the IPO contribution in the tropical Pacific to verify if the origin of the residual is externally forced signal or a signal due to internal climate modes of variability. To do so, we use two approaches: (1) a simple Empirical Orthogonal Function (EOF) analysis on the residual altimetry signal without IPO and (2) comparison of the residual signal with CMIP5 based climate models.

2. Data and methods

2.1. Satellite altimetry sea level (1993–2013)

In this study, we used the altimetry-based 2D gridded sea level anomalies from AVISO. This data is available on a weekly interval as a ¼° regular grid from January 1993 to December 2013. This is the DT-MSLA 'Ref'

series computed at Collecte Localisation Satellite (CLS) by merging several altimeter missions namely: Topex/Poseidon, Jason-1 and Jason-2, Envisat, ERS-1 and ERS-2. This dataset has undergone geophysical and orbital corrections. Detailed information on the dataset and processing can be found in Ablain *et al* (2009). In order to be consistent with the other data sets used in this study, the altimetry sea level data at weekly intervals has been averaged to a monthly scale. The annual and semi-annual signals have been removed through a least-square fit of twelve and six month period sinusoids. Since the focus of our study is regional sea level trend patterns, the uniform global mean sea level has been removed from the altimetry data.

The contribution of decadal climate variability (i.e. IPO) to sea level can be derived from a regression of the climatic index on sea level (Palanisamy *et al* 2015). Here we make use of an updated version of the IPO index available from 1871 until mid-2014 (kindly provided by C K Folland). This index is similar to that of PDO which is defined as the leading principal component of the North Pacific (poleward of 20°N) monthly sea surface temperature (SST) variability (Mantua *et al* 1997, Mantua and Hare 2002, Zhang *et al* 1997). The IPO is the Pacific-wide equivalent of the PDO, with as much variance in the Southern Hemisphere Pacific (at least to 55°S) as in the Northern Hemisphere (Folland *et al* 1999). Using the IPO index, we perform a multiple linear regression of IPO and its corresponding Hilbert transform on altimetry based observed sea level. The Hilbert transform will also take the phase of the IPO associated with propagating signal into account (Palanisamy *et al* 2015). The IPO contributed sea level signal obtained as a result is then removed from the observed altimetry-based sea level.

2.2. 2D past sea level reconstruction (1960–2013)

The limited time length of the altimetry data can become an issue when evaluating low frequency variability in terms of trends (Frankcombe *et al* 2014). IPO is a low frequency natural climate oscillation with a periodicity of around two to three decades. Several studies (Deser *et al* 2004, Yasunaka and Hanawa 2003, Hare and Mantua 2000) have shown evidence of four IPO phase changes since the 20th century: two warm phases during 1925–1946, 1977–1997 and two cold phases during 1947–1976 and since 1998. Performing regression of IPO index on the observed altimetry sea level signal since 1993 implies that we take into account only one complete phase of the IPO climate mode, i.e., the current negative IPO phase since 1998. This can result in trend aliasing (Frankcombe *et al* 2014), i.e. the incomplete separation of the trend and low frequency IPO variability since the period of the internal variability is longer than the altimetry period. The inability to distinguish between the trend and low frequency variability results in the low frequency variability itself to be aliased as a trend. Frankcombe *et al* (2014) have shown that around 50 years of time series is required to extract low frequency variability from the sea level signal. However, it is to be noted that exact quantification of signal related to internal variability using finite records still remains a challenge. For example, Wittenberg (2009) has shown that there is no guarantee that 150 year historical SST records can be used to determine a full representative for ENSO modulation. Furthermore, Bordbar *et al* (2015) have mentioned that the lack of long-term observations poses a challenge in quantifying long-term internal variability as it can introduce considerable uncertainty on the future evolution of regional sea level.

In our study, in order to verify if the residual trend pattern in the tropical Pacific after having removed the IPO contribution from altimetry sea level is due to aliasing effect or not, we also used the updated version of a 2D past sea level reconstruction from Meyssignac *et al* (2012a) available from 1960 to 2013. This 2D past sea level reconstruction is an optimal interpolation of long tide gauge records with Empirical Orthogonal Function (EOF) deduced from the sea level output of 3 different ocean reanalyses, namely GECCO2 (Köhl, 2015), SODA 2.1.6 (Carton and Giese 2008) and ORAS4 (Balmaseda *et al* 2013). This approach uses EOFs to combine 134 long tide gauge records of limited spatial coverage and 2D sea level patterns based on ocean reanalysis. Three different past sea level reconstructions based on EOFs from each ocean reanalysis were performed and then merged in a unique mean reconstruction following Meyssignac *et al* 2012a. Compared to previous reconstructions available in the literature, these updated reconstructions are not global reconstructions based on global EOFs. They are based on regional reconstructions over the Pacific-Indian Basin and the Atlantic Basin which were further concatenated into global reconstructions. By separating the Indian-Pacific region from the Atlantic region, it is expected that EOFs are more consistent with the regional climate modes of the basins (ENSO and PDO in the Indo-Pacific region and NAO in the Atlantic) to interpolate the tide gauge records. It yields a better reconstruction of the sea level over the last decades in comparison with independent tide gauge records (see Meyssignac *et al* 2015).

The linear regression of IPO is then performed on this data with a time length of 53 years and IPO contribution is then removed from the reconstruction-based sea level signal. Comparison of reconstruction based residual trend pattern with altimetry-based residual trend pattern over 1993–2013 would reveal the presence of aliasing if any.

2.3. CMIP5 climate models (1860–2098)

To investigate changes in sea level due to external forcing, we also analyzed the dynamic sea surface

Table 1. List of CMIP5 dynamic sea level models and the corresponding number of realizations used in the study.

Dynamic sea level data	
CMIP5 models	No. of realizations
ACCESS1.0	1
ACCESS1.3	1
CanESM2	5
CCSM4	6
CNRM-CM5	5
CSIRO-Mk3.6.0	10
GFDL-CM3	1
GFDL-ESM2M	1
HadGEM2-CC	1
HadGEM2-ES	4
INM-CM4	1
IPSL-CM5A-LR	4
IPSL-CM5A-Mr	1
MIROC5	3
MIROC-ESM	1
MIROC-ESM-CHEM	1
MPI-ESM-LR	3
MPI-ESM-Mr	1
MRI-CGCM3	1
NorESM1-M	1
NorESM1-ME	1
Total no. of realizations	53
Total no. of models	21

height from 21 climate models from CMIP5 (Taylor *et al* 2012). Table 1 displays the list of CMIP5 models used. The dynamic sea surface height includes changes in the thermohaline and wind-driven circulations (Richter and Marzeion 2014). The CMIP5 climate models do not include the net ocean mass changes from melting ice sheets and glaciers as well as associated gravitational and solid earth responses. But this term is almost uniform over the last 20 years and likely negligible (Landerer *et al* 2014, Yin *et al* 2010) in terms of spatial variability in regional sea level trends. Hence it is not important for our study. We used the historical 'all forcing' CMIP5 climate simulations available from 1850/1860. These simulations are forced by natural forcing agents (solar radiation, volcanic aerosols) and anthropogenic forcing agents (e.g. greenhouse gas, anthropogenic aerosols, and ozone etc, Taylor *et al* 2012). CMIP5 historical simulations in general end in 2005. Since our period of interest corresponds to that of the satellite altimetry era from 1993 until 2013, we therefore extended the historical simulations by concatenating the 21st century projections under the Representative Concentration Pathway (RCP) 8.5 scenario (2006–2098/2100) to the historical simulations. The RCP8.5 scenario assumes continuous anthropogenic GHG emission throughout the 21st century and can also be considered as a representative of the present scenario (IPCC 2013).

Among the 21 models, some models provide multiple realizations of the historical experiment. For example, CMIP5 historical runs initialized from different times of a control run would be identified as 'r1','r2', etc. The RCP simulation is assigned the same realization number as the historical run from which it was initiated (information on CMIP5 data reference syntax can be found at http://cmip-pcmdi.llnl.gov/cmip5/output_req.html). In our study, all possible realizations that correspond to the Historical+RCP8.5 simulations were taken into account (see table 1). As a result, 53 realizations were used in this study. The data is at yearly resolution and the spatial fields are remapped to a regular $1^\circ \times 1^\circ$ resolution. All climate models are corrected for the model drift (Gregory *et al* 2001, Sen Gupta *et al* 2012) by removing the quadratic trend in the time series of the accompanying pre-industrial control run. The global mean was removed from the dynamic sea level data at every time step.

The temporal phases of the internal climate variability in the CMIP5 models are not reproduced. This is because in Global Coupled Models (GCMs), the unforced internal climate modes (e.g. ENSO, IPO) are not constrained to be synchronized to real-world occurrence (Landerer *et al* 2014). Furthermore, the ability of climate models to accurately reproduce the internal climate modes has been a questionable subject. Since the interest of this study is to look for externally forced sea level signals, performing a multi-model ensemble (MME) of several such CMIP5 models will in general average out/reduce signals related to internal climate variability thereby reflecting the forced signal mostly due to external forcings. To avoid bias to models with more realizations, in this study, the realizations of each model are first averaged to obtain the model mean and then the 21 models are averaged (as in Yin, 2012).Taking into account one realization per model (instead of averaging all realizations of each model first) produces the same results.

3. Results

3.1. Observation based Pacific Ocean sea level trend pattern and internal climate modes

Figure 1(a) displays the observed altimetry based sea level spatial trend pattern over 1993–2013 (with the global mean sea level (GMSL) removed) and figure 1 (b) displays the contribution of IPO to Pacific Ocean sea level trend over 1993–2013 based on the regression of IPO index on sea level signal. Stippling indicates regions where the trends are non-significant (p-value > 0.05). The IPO contributed sea level trend pattern exhibits similar broad scale positive v-shaped trend pattern and east-west tropical dipole as the observed altimetry-based sea level trend pattern. This trend pattern is also similar to the decadal sea level fingerprint of Zhang and Church (2012) (see their figure 4(b)) and the PDO contributed sea level trend

pattern of Hamlington *et al* (2014a) (see their figure 1 (b)). Their methodology of calculation of the decadal sea level fingerprint somewhat differs from the methodology used in this study. Zhang and Church (2012) used multiple variable linear regression (defining 'new' interannual and decadal climatic indices based on PDO and Multivariate ENSO Index (MEI)) to discriminate the interannual, decadal and longer term trend. On the other hand, Hamlington *et al* (2014a) estimated the PDO contribution by an EOF analysis of sea level reconstruction (Hamlington *et al* 2014b) based 20 year trend patterns from 1950 to 2010. Based on the results obtained in this study and studies of Zhang and Church (2012) and Hamlington *et al* (2014a), we can observe that the IPO contributed observed sea level spatial trend pattern is hardly sensitive to the methodologies used.

Observed altimetry-based sea level trend pattern without IPO contribution (figure 2(a)) and henceforth called the (Alti-IPO) residual signal, is estimated by subtracting the IPO contributed sea level signal from the altimetry based sea level signal. The Alti-IPO sea level trend pattern is insignificant in most of the regions of the Pacific Ocean with exceptions in the western tropical and southern central Pacific. Though weaker, the positive trend pattern in the western tropical Pacific (especially near 10°N/S) is in the order of 2–4 mm yr^{-1}. The residual sea level trend pattern is similar to figure 1(c) of Hamlington *et al* (2014a) that has been attributed to an anthropogenic sea level fingerprint.

In order to verify if the residual trend pattern is due to aliasing of IPO and sea level signal as a result of short time length of study, we used the 2D reconstruction based Pacific Ocean (until 40°S latitude as the reconstruction data is not available further south) sea level spatial trend pattern over 1993–2013 without IPO contribution (figure 2(b)). As described in section 2.2, this is obtained by performing a regression of IPO on reconstruction based sea level signal over 53 years and removing its contribution. The residual trend patterns in both figure 2(a) (Alti-IPO) and figure 2(b) (reconstruction-IPO) at the region of interest, i.e the western tropical Pacific are very similar. This implies that the trend pattern of the Alti-IPO residual signal is likely not a result of the aliasing effect.

3.1.1. Analysis of Alti-IPO residual signal

As the next step, we tried to verify if Alti-IPO residual pattern can be related to any physical processes. So an EOF analysis was first performed on the Alti-IPO residual signal and the mode with the maximum variance was analyzed. Figures 3(a) and (b) show the spatial pattern and corresponding temporal curve of the first EOF mode of Alti-IPO sea level signal, respectively. The maximum variance explained by the first EOF mode of the Alti-IPO residual is only 6%. Performing an EOF analysis directly on the Pacific Ocean observed altimetry based sea level results in a first mode with a variance of 17% (not shown here). The reduction in the maximum variance explained by the Alti-IPO EOF implies the significant role of IPO in the Pacific Ocean sea level. From figure 3(a), we can observe that the spatial pattern very closely resembles the central Pacific ENSO event, also called the El Niño Modoki. While conventional El Niño is characterized by strong anomalous warming in the eastern tropical Pacific, El Niño Modoki is associated with strong anomalous warming in the central tropical Pacific and cooling in the eastern and western tropical Pacific (Ashok *et al* 2007, also see figure 14 of Bosc and Delcroix (2008)).

The temporal curve that corresponds to EOF1 was then analyzed. Firstly, it was correlated with the El Niño Modoki Index (EMI). The index is calculated as the area averaged sea surface temperature anomaly (SSTA) over 3 regions: (1) 165°E–140°W, 10°S–10°N, (2) 110°W–70°W, 15°S–5°N, and (3) 125°E–145°E, 10°S–20°N (see Ashok *et al* (2007) for more details). Over 1993–2013, we find a correlation of 0.7 between the temporal curve and the EMI index. If we consider only the time period between 1993 and 2008 (since from figure 3(b), we can observe deterioration between the two temporal curves after 2008), the correlation increases to 0.8. The correlations are all significant at the 95% confidence level. One possible reason for the deterioration of correlation after 2008 (correlation $= -0.2$) could be related to the occurrence of two extreme La Niña events (2007–2008 and 2010–2011). However this needs to be further investigated. Even though this mode represents only 6% of the total variance, it can have an impact on sea level trends. For example, the positive trend observed in the temporal curve between 2004 and 2008/2009 is related to the period of El Niño Modoki events (see figure 1 of Singh *et al* (2011)). As a result, during this time period, the central tropical Pacific experienced increased sea level rates.

On performing a power spectral analysis on the EOF1 temporal curve over 1993–2013, we obtain a periodicity of approximately 3 years. This corresponds to the periodicity of ENSO events that ranges between 3 and 8 years.

The presence of El Niño Modoki signal in the Alti-IPO residual indicates that there is in fact some ENSO-related (in specific El Niño Modoki until 2008) internal variability still remaining even after the removal of IPO.

3.1.2. Analysis of Alti-IPO-EMI residual signal

To further analyze the residual trend pattern, we then removed the El Niño Modoki contributed signal from the Alti-IPO residual signal (henceforth called Alti-IPO-EMI) by once again performing a linear regression of EMI on Alti-IPO. Figure 4 displays the sea level spatial trend pattern in the Pacific Ocean from observed altimetry without IPO and El Niño Modoki related internal variability. On comparison with Alti-

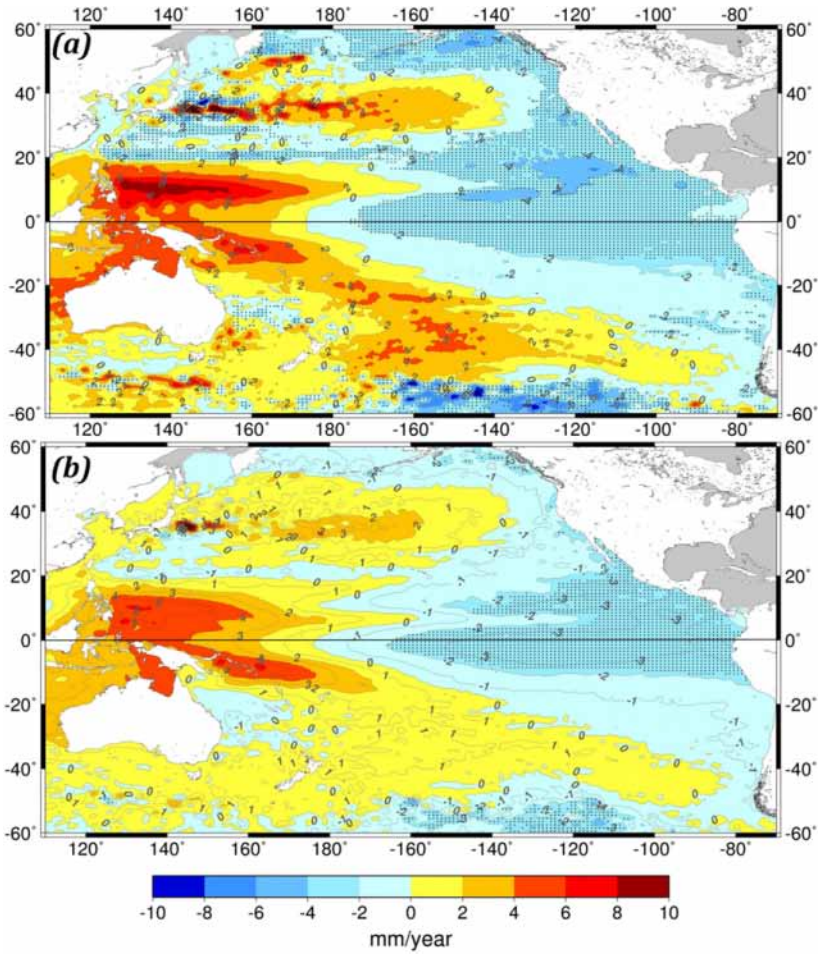

Figure 1. (a) Observed altimetry based sea level spatial trend pattern and (b) IPO contributed sea level spatial trend pattern (uniform global mean has been removed) in the Pacific Ocean over 1993–2013. Stippling indicates regions of non-significant trend (p-value $>$ 0.05).

IPO residual sea level trend pattern in figure 2(a), we can observe that the removal of the El Niño Modoki signal from Alti-IPO results only in a small decrease in magnitude of the residual sea level trend with no significant changes in the trend pattern. Furthermore, in figure 4, we can observe meridionally alternating positive and negative sea level trend patterns within 20°N and 20°S with mostly positive trend patterns at the equatorial band. These patterns suggest accumulation of a warm water volume in the equatorial band and a reduction in the north and south equatorial counter currents which all together are a reminiscent of a strong El Niño situation (Meinen and McPhaden 2000, Kessler and Taft 1987). However, since the trend patterns in this region are not significant, it is difficult to have a robust conclusion on this. An EOF analysis on the Alti-IPO-EMI sea level signal results in the first EOF mode closely resembling the eastern Pacific ENSO event in terms of spatial pattern (figure 5(a)) with the evident strong 1997/1998 El Niño event clearly visible in the temporal curve (figure 5(b)). The periodicity of the temporal curve is around 3–4 years and this once again corresponds to the ENSO periodicity.

All the above discussed results show that attempts to separate/remove both decadal and interannual climate modes from observed altimetry based sea level signal through the method of linear regression (as shown in this study) or the methodology of Hamlington *et al* (2014a) do not in fact totally eliminate the internal sea level variability. Some non-linear internal variability related to intense ENSO events such as the 1997/1998 El Niño still remains in the residual.

3.2. CMIP5 model based sea level spatial trend pattern and internal climate modes

3.2.1. Multi model ensemble (MME) and internal climate modes

As mentioned in section 2.3, performing a Multi Model Ensemble (MME) of the 21 CMIP5 models would in general average out/reduce sea level signal due to internal climate modes. The MME containing only the expected sea level response to external forcings (natural and anthropogenic) can then be compared with the Alti-IPO and Alti-IPO-EMI residual sea level trend patterns. If the sea level spatial trend pattern of MME is similar to that of the above mentioned two residual trend patterns, we can

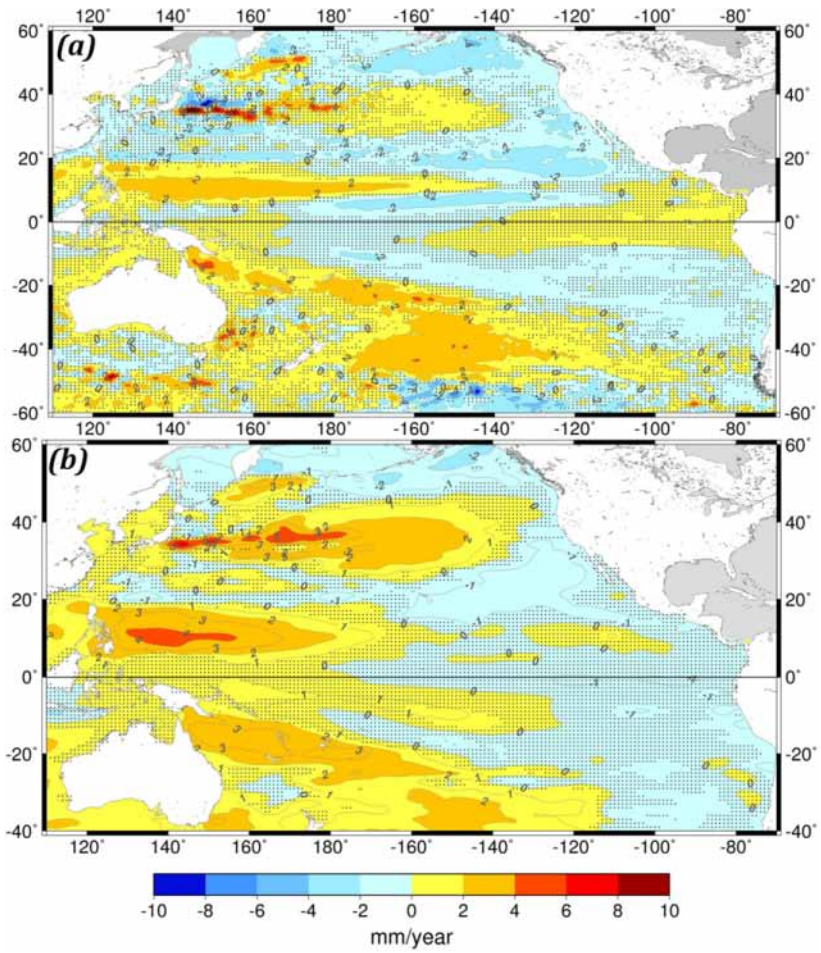

Figure 2. (a) Altimetry and (b) 2D reconstruction-based Pacific Ocean sea level spatial trend pattern without IPO over 1993–2013 (uniform global mean has been removed from both before performing the regression. In the case of 2D reconstruction, regression was performed over 1960–2013 and the result is plotted over 1993–2013). Stippling indicates regions of non-significant trend (p-value $>$ 0.05).

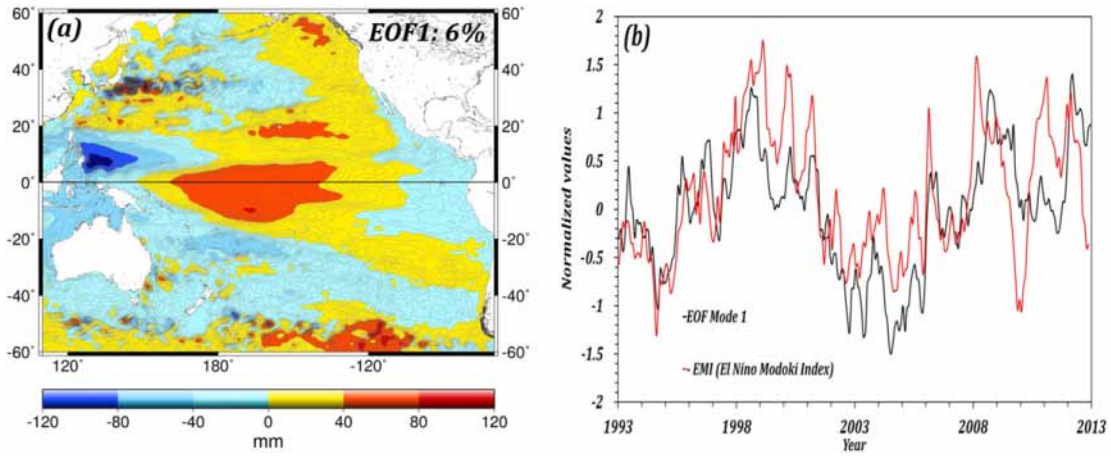

Figure 3. (a) Spatial pattern and (b) its corresponding time curve of the first EOF mode of Altimetry-IPO residual signal over 1993–2013. The EMI index is represented as the red curve.

conclude the presence of externally forced sea level signal in the Pacific Ocean over the 2 recent decades.

Before a direct comparison of the sea level trend patterns, the presence of any internal climate modes in the MME was first verified. EOF decomposition was performed on the MME-based sea level signal between 1900 and 2098, and the corresponding spatial and temporal patterns were studied. Even though the main

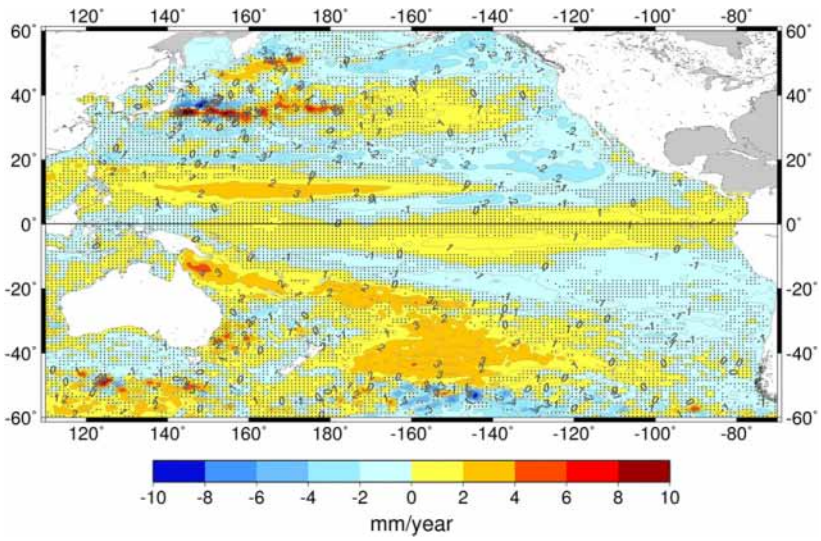

Figure 4. Altimetry based Pacific Ocean sea level spatial trend pattern without IPO and EMI contribution over 1993–2013. Stippling indicates regions of non-significant trend (p-value $>$ 0.05).

region of interest of our study is the Pacific Ocean, for this verification, we chose the global ocean. This would enable us to verify the effectiveness of MME in reducing the impact of internal climate modes not only in the Pacific but also in the other oceans. Furthermore, such verification would also give us an idea on regions where the impact of external forcing is the maximum and the structure of their corresponding spatial patterns.

Figure 6(a) and the black curve in figure 6(b) display the spatial pattern and temporal curve of the first EOF mode of the MME sea level with total variance of 96%. The second and third EOF modes contribute 3% and 1% of the total variance and do not exhibit any significant spatial patterns or temporal curves (not shown here). From figure 6(b), we can observe that the temporal curve is almost flat until 1970 after which there is an increase that continues over time implying an accelerated dynamic sea level change. Skeie *et al* (2011) (figure 1(a)) and Myhre *et al* (2013) (figure 8.18) have shown that the radiative forcing from CO_2 and other well-mixed greenhouse gases (WMGHG) has rapidly increased since the 1950s with the CO_2 emission being the largest contributor to the increased anthropogenic forcing since 1960s. These are in agreement with the time series in figure 6(b) showing an increased signal since 1970.

In terms of spatial pattern, this increase in sea level appears in the northern high latitudinal band between 70°N and 85°N, North Atlantic Ocean south of Greenland between 30°N and 60°N and also in the southern latitudinal band between 40°S and 45°S. Regions of positive sea level patterns also occur in the western extra-tropical Pacific Ocean between 30°N and 40°N and in western Indian and central Atlantic oceans. Region of negative sea level change appears in the Southern Ocean beyond the 50°S latitudinal band. This is in agreement with the results from Bilbao *et al* (2015). Performing the same EOF analysis only on the Pacific Ocean (boxed region in figure 6(a)), we obtain the same Pacific Ocean spatial pattern (with a variance of 93%) as in figure 6(a). The temporal curve that corresponds to the Pacific Ocean first EOF mode (blue curve in figure 6(b)) is very similar to that of the global EOF1 temporal curve. On close observation of both EOF1 temporal curves, we can also notice that while the global curve exhibits small amplitude oscillations, the curve corresponding to the Pacific Ocean exhibits higher amplitude oscillations throughout the time period. Presence of oscillations in both the curves which do not correspond to oscillations in the external forcing (due to volcanic forcing or solar forcing) indicates that performing the multi-model mean may not average out the entire signal that corresponds to internal variability and there may still remain some residual internal variability. Since, in general the internal variability exhibits stronger amplitude oscillations regionally than globally, even the residual of the Pacific Ocean internal variability obtained (blue curve in figure 6(b)) tends to be greater at regional scale.

In order to effectively obtain the temporal curve and spatial pattern that corresponds to external forcing only, we performed a spline smoothing (Ribes *et al* 2010) on the global EOF1 temporal curve to remove the small amplitude oscillations. The smoothed temporal curve (red dotted curve in figure 6(b) with an upward offset of 0.1 for clarity) is then regressed on to the CMIP5 MME sea level dataset and the sea level pattern that corresponds to the smoothed temporal curve is obtained. On calculating the variance, the CMIP5 MME sea level signal thus obtained after regression (hereafter called regressed CMIP5 MME) explains 97% of the total CMIP5 MME signal. The regressed CMIP5 MME sea level signal can

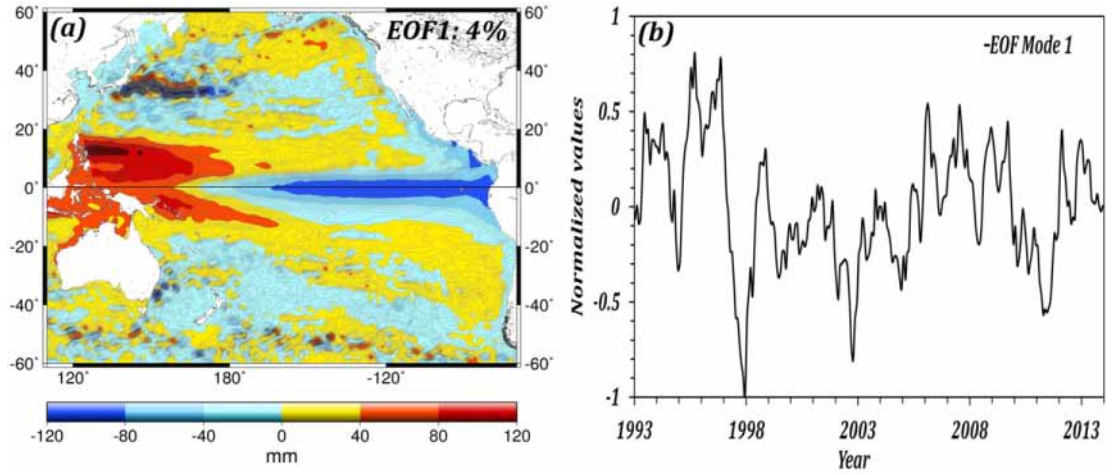

Figure 5. (a) Spatial pattern and (b) its corresponding time curve of the first EOF mode of Altimetry-IPO-EMI residual signal over 1993–2013.

now be considered to contain mainly externally forced sea level signal.

3.2.2. MME-based sea level spatial trend pattern over altimetry period

As mentioned in section 3.2.1, the regressed CMIP5 MME sea level signal that contains mainly externally forced signal can be compared with Alti-IPO and Alti-IPO-EMI residual sea level spatial trend patterns to verify if the two latter residual patterns are linked to external forcing. Figure 7 displays the regressed MME-based sea level spatial trend pattern in the Pacific Ocean between 1993 and 2013. Stippling indicates regions where the trends are insignificant (p-value > 0.05). The externally forced sea level spatial trend pattern is positive in the north-west and south-west Pacific Ocean between the sub-tropical latitudes of 20°N–40°N and 20°S-40°S. In the north-west Pacific, the positive trend values are in the order between 0.2 mm yr^{-1} and 0.7 mm yr^{-1} while in the south-west the trend values range between 0.2 mm yr^{-1} and 1.6 mm yr^{-1}. Interestingly, from the Alti-IPO (figure 2(a)) and Alti-IPO-EMI (figure 4) residual patterns, we can clearly notice that in the western tropical Pacific, the residual sea level trend patterns are not comparable with the regressed CMIP5 MME based trend pattern in figure 7 (Note that the color scale is not the same as in figure 2(a) and 4). Contrary to the Alti-IPO and Alti-IPO-EMI trend patterns, the positive trend pattern that appears in the western tropical Pacific extending towards the east between 10°N to 20°N and 120°E to 120°W is only in the range of 0.1 mm yr^{-1} to 0.3 mm yr^{-1}. The absence of significantly high positive sea level trend in the western tropical Pacific over the altimetry era from the regressed CMIP5 MME based data shows that the residual trend patterns observed in the altimetry signal after having removed IPO and EMI contribution is not consistent with the CMIP5 MME based expected sea level response to external forcing. This once again suggests that the residual Alti-IPO/ Alti-IPO-EMI patterns cannot be attributed to anthropogenic signal. However in the Pacific Ocean east of the Australian continent between 20°S and 40°S latitudes, we can observe that the Alti-IPO and Alti-IPO-EMI trend patterns are consistent with that of the CMIP5 MME. This indicates the possible sea level response to external forcing in this region.

3.3. Discussion and conclusion

Several earlier studies (e.g. Zhang and Church 2012, McGregor *et al* 2007, Verdon and Franks 2006, Power *et al* 2006 Deser *et al* 2004, Mantua and Hare 2002) have tried to understand and explain the relation between ENSO and IPO/PDO. They have shown that PDO/IPO is essentially the low frequency residual of ENSO variability occurring at multi-decadal time scales. Furthermore, Verdon and Franks, (2006) have shown that an increased occurrence of El Nino events during positive phase of PDO/IPO whereas negative PDO/IPO triggers more La Niña events.

While the above mentioned studies have shown that PDO/IPO and ENSO are inter-related, several studies (e.g. Schneider and Cornuelle 2005, Pierce 2001) have also shown that the former is not a mode of variability linked only to ENSO but is a blend of several other phenomena like the zonal advection in the Kuroshio-Oyashio Extension, Aleutian low anomalies and others. All these studies lead us to question if attempts to remove the decadal natural climate mode (PDO/IPO, if assumed that they are adequately sampled using existing historical and observational records) from the sea level signal could also effectively remove all other internal natural climate modes.

In this study, we analyzed the observed altimetry based sea level spatial trend patterns in the Pacific Ocean after having removed IPO contribution through linear regression. On performing a simple

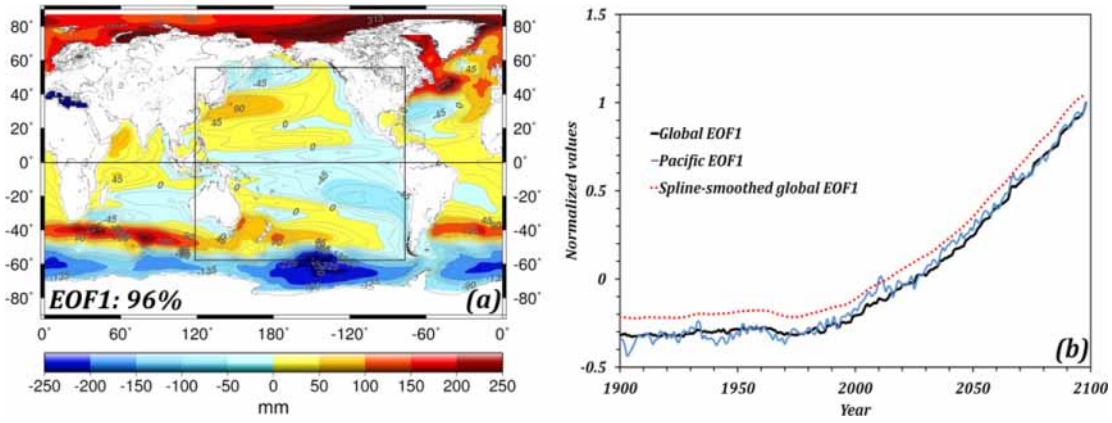

Figure 6. (a) Spatial pattern of the first EOF mode of CMIP5 MME sea level over 1900–2098; (b) its corresponding temporal curve (black curve). The red dotted curve corresponds to the spline-smoothed EOF1 temporal curve (with an upward offset of 0.1 for clarity) and the blue curve corresponds to the Pacific Ocean EOF1 temporal curve estimated over the boxed region in (a).

EOF analysis on the residual (Alti-IPO) sea level signal, we found the presence of ENSO-related El Nino Modoki (Central Pacific) signal in the residual. Further efforts to remove the El Niño Modoki signal from Alti-IPO signal through linear regression still resulted in the presence of Eastern Pacific ENSO signal in the residual. This indicates that linearly regressing IPO on observed sea level and removing its contribution does not totally remove the entire internal sea level variability. Nonlinear ENSO-related variability that does not linearly co-vary with IPO still remains in the residual sea level signal. Our results show that the methodology of removing the main decadal natural climate mode from sea level signal and analyzing the residual is not an effective way to explain the contribution of external anthropogenic sea level fingerprint.

The range of altimetry-based regional sea level trend uncertainties/error estimate should also be considered in these studies as the residual sea level trend pattern after removing IPO and ENSO contributions should be compared to the pattern of uncertainty. A detailed comparison is beyond the scope of this study as further investigations are needed to obtain accurate altimetry-based trend error patterns at regional scale. However we expect that the patterns of regional altimetry error do not coincide to those in figure 2(a) (Alti-IPO) and figure 4 (Alti-IPO-EMI) as the errors are mainly large spatial patterns at hemispherical scale in the order of 2 mm yr^{-1} to 3 mm yr^{-1} with orbital errors contributing the most (Ablain *et al* 2015, Couhert *et al* 2015).

Furthermore, regressed CMIP5 MME-based sea level spatial trend pattern in the tropical Pacific over the altimetry period do not display any positive sea level trend values that are comparable to the altimetry based sea level signal after having removed the contribution of the decadal natural climate mode. This suggests that the residual positive trend pattern observed in the western tropical Pacific is not externally forced and thereby not anthropogenic in origin. In addition the amplitude of the sea level spatial trend pattern from regressed CMIP5 MME is low over the altimetry period in the tropical Pacific. This amplitude is significantly lower than the expected error in trend patterns from satellite altimetry (in the order of 2 mm yr^{-1} to 3 mm yr^{-1}, Ablain *et al* 2015, Couhert *et al* 2015) and suggest that satellite altimetry measurement is still not accurate enough to detect the anthropogenic signal in the 20 year tropical Pacific sea level trends.

Our results are also in agreement with studies of Richter and Marzeion (2014), Lyu *et al* (2014), Jordà (2014), Frankcombe *et al* (2014), Bilbao *et al* (2015) who have shown that in regions of high internal variability, the trend due to externally forced signal is masked during longer time spans than in regions of low internal variability. This is the case of tropical Pacific which is a region highly impacted by internal variability. Studying the residual sea level signal after separating/removing the internal climate modes over a short time period of 20 years in this region may not yield significant results with respect to external forcing. This is also in agreement with Meyssignac *et al* (2012b) who have shown that over the 17 years altimetry period, the tropical Pacific observed sea level spatial trend pattern is mainly due to internal variability.

Our study suggests that detection/attribution studies should be focused on other regions such as Northern and Southern Oceans, North Atlantic, Southern Pacific to the east of Australia. Based on CMIP5 MME (see figures 6 and 7), these are the regions that show significant externally forced sea level signals. Detailed studies on these regions could help us understand the role of externally forced signal on sea level.

Lastly, another important factor to consider would be the impact of external anthropogenic forcing on the natural internal climate modes. In the previous studies (Hamlington *et al* 2014b, Palanisamy *et al* 2015) and this current study, it has been assumed that the natural

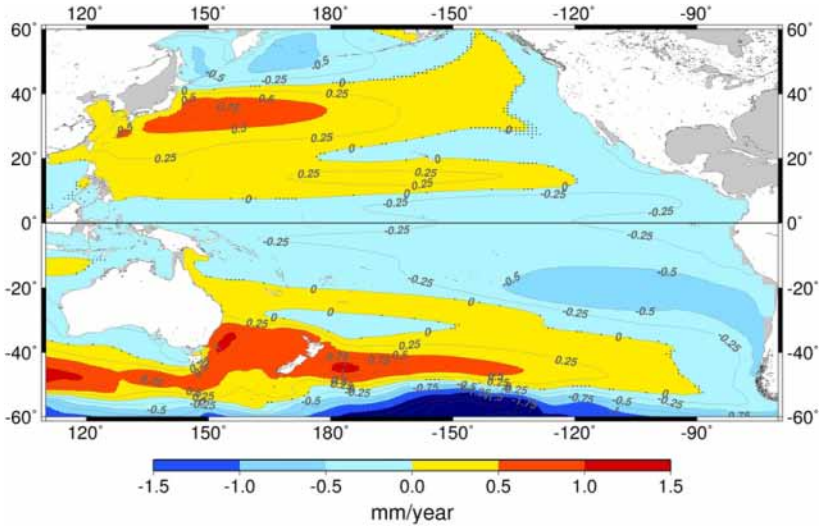

Figure 7. Pacific Ocean sea level spatial trend pattern estimated from regressed CMIP5 MME sea level data over 1993–2013. Stippling indicates regions of non-significant trend (p-value $>$ 0.05).

internal climate mode is independent of the external anthropogenic forcing. Attempts have then been made to separate/remove the internal climate mode from the sea level signal and attribute the residual to be anthropogenic in origin. However it should not be forgotten that the anthropogenic global warming signal may not only appear as a constant increasing pattern in response to greenhouse gas emissions (as seen in figure 6(b)) but could also change the behavior of the internal climate modes. Recently, using CMIP5 models, Dong *et al* (2014) have shown that in the twentieth century, the Pacific Decadal Variability is not only dominated by internal variability but also significantly affected by external forcing (combined effects of greenhouse gases and anthropogenic aerosols). While the greenhouse gas forcing induces strong surface downward shortwave radiation over the tropical Pacific resulting in stronger warming, the anthropogenic aerosol forcing induces stronger cooling in the North Pacific due to reduced surface downward shortwave radiation (Dong *et al* 2014). Furthermore, in terms of ENSO events, studies such as Cai *et al* (2015), Cai *et al* (2014), Power *et al* (2013 and references therein) have shown an increase in the frequency of extreme El Niño and La Niña events occurring due to increasing greenhouse warming while Yeh *et al* (2009) show an increase in El Niño Modoki events. Though possibly model dependent, all the above mentioned studies show the role of external anthropogenic forcing on internal climate modes. Therefore by removing/separating the internal climate mode from sea level signal, it is highly probable that we also remove a part of (if not all) the external anthropogenic forcing.

This also indicates that we cannot totally deny the role of external forcing in the western tropical Pacific sea level changes over the two recent decades. Indeed the recent sea level intensification in this region could be a result of very high internal variability driven by intensified trade winds which could have partly been driven by the anthropogenic forcing itself (e.g. England *et al* 2014). Therefore in future, it is important to first understand how anthropogenic forcing can impact the mechanisms that drive the internal climate modes.

Acknowledgments

We thank Dr Aurelien Ribes for his useful suggestions on CMIP5 models analysis. We also thank the anonymous reviewers for their comments and suggestions. We acknowledge AVISO for making available the satellite altimetry sea level product. We also acknowledge the World Climate Research Programme's Working Group on Coupled Modelling, which is responsible for CMIP5 and we thank the climate modeling groups for producing and making available their model output. Support for CMIP5 is provided by the US Department of Energy. H Palanisamy is supported by a CNES/CLS PhD grant.

References

Ablain M *et al* 2015 Improved sea level record over the satellite altimetry era (1993–2010) from the climate change initiative project *Ocean Sci* **11** 67–82

Ablain M, Cazenave A, Valladeau G and Guinehut S 2009 A new assessment of the error budget of global mean sea level rate estimated by satellite altimetry over 1993–2008 *Ocean Sci.* **5** 193–201

Ashok K, Behera S K, Rao S A, Weng H and Yamagata T 2007 El Niño Modoki and its possible teleconnection *J. Geophys. Res. Oceans* **112** C11007

Balmaseda M A, Mogensen K and Weaver A T 2013 Evaluation of the ECMWF ocean reanalysis system ORAS4 *Q. J. R. Meteorol. Soc.* **139** 1132–61

Bilbao R A F, Gregory J M and Bouttes N 2015 Analysis of the regional pattern of sea level change due to ocean dynamics

and density change for 1993–2099 in observations and CMIP5 AOGCMs *Clim. Dyn.* 1–20
Bordbar M H, Martin T, Latif M and Park W 2015 Effects of long-term variability on projections of twenty-first century dynamic sea level *Nat. Clim. Change* **5** 343–7
Bosc C and Delcroix T 2008 Observed equatorial Rossby waves and ENSO-related warm water volume changes in the equatorial Pacific Ocean *J. Geophys. Res. Oceans* **113** C06003
Bromirski P D, Miller A J, Flick R E and Auad G 2011 Dynamical suppression of sea level rise along the Pacific coast of North America: indications for imminent acceleration *J. Geophys. Res. Oceans* **116** C07005
Cai W *et al* 2014 Increasing frequency of extreme El Nino events due to greenhouse warming *Nat. Clim. Change* **4** 111–6
Cai W *et al* 2015 Increased frequency of extreme La Nina events under greenhouse warming *Nat. Clim. Change* **5** 132–7
Carton J A and Giese B S 2008 A reanalysis of ocean climate using simple ocean data assimilation (SODA) *Mon. Weather Rev.* **136** 2999–3017
Cazenave A and Cozannet G L 2014 Sea level rise and its coastal impacts *Earths Future* **2** 15–34
Church J A *et al* 2013 Sea level change *Climate Change 2013: The Physical Science Basis. Contribution of Working Group I to the Fifth Assessment Report of the Intergovernmental Panel on Climate Change* ed T F Stocker, D Qin, G-K Plattner, M Tignor, S K Allen, J Boschung, A Nauels, Y Xia, V Bex and P M Midgley (Cambridge, United Kingdom:: Cambridge University Press)
Couhert A, Cerri L, Legeais J-F, Ablain M, Zelensky N P, Haines B J, Lemoine F G, Bertiger W I, Desai S D and Otten M 2015 Towards the 1 mm/y stability of the radial orbit error at regional scales *Adv. Space Res.* **55** 2–23
Deser C, Phillips A S and Hurrell J W 2004 Pacific interdecadal climate variability: linkages between the tropics and the north pacific during boreal winter since 1900 *J. Clim.*, **17** 3109–24
Dong L, Zhou T and Chen X 2014 Changes of Pacific decadal variability in the twentieth century driven by internal variability, greenhouse gases, and aerosols *Geophys. Res. Lett.* **41** 8570–7
England M H, McGregor S, Spence P, Meehl G A, Timmermann A, Cai W, Gupta A S, McPhaden M J, Purich A and Santoso A 2014 Recent intensification of wind-driven circulation in the Pacific and the ongoing warming hiatus *Nat. Clim. Change* **4** 222–7
Folland C K, Parker D E, Colman A and Washington R 1999 Large scale modes of ocean surface temperature since the late nineteenth century Refereed book: ch 4, pp 73–102 *of Beyond El Nino: Decadal and Interdecadal Climate Variability* ed A Navarra (Berlin: Springer)
Frankcombe L M, McGregor S and England M H 2014 Robustness of the modes of Indo-Pacific sea level variability *Clim. Dyn.* 1–18 doi:10.1007/s00382-014-2377-0
Fukumori I and Wang O 2013 Origins of heat and freshwater anomalies underlying regional decadal sea level trends *Geophys. Res. Lett.* **40** 563–7
Gregory J M *et al* 2001 Comparison of results from several AOGCMs for global and regional sea-level change 1900–2100 *Clim. Dyn.* **18** 225–40
Hamlington B D, Strassburg M W, Leben R R, Han W, Nerem R S and Kim K-Y 2014a Uncovering an anthropogenic sea-level rise signal in the Pacific Ocean *Nat. Clim. Change* **4** 782–5
Hamlington B D, Leben R R, Strassburg M W and Kim K-Y 2014b Cyclostationary empirical orthogonal function sea-level reconstruction *Geosci. Data J.* **1** 13–9
Han W *et al* 2013 Intensification of decadal and multi-decadal sea level variability in the western tropical Pacific during recent decades *Clim. Dyn.* 1–23 doi:10.1007/s00382-013-1951-1
Hare S R and Mantua N J 2000 Empirical evidence for North Pacific regime shifts in 1977 and 1989 *Prog. Oceanogr.* **47** 103–45
IPCC 2013 *Climate Change 2013: The Physical Science Basis. Contribution of Working Group I to the Fifth Assessment Report of the Intergovernmental Panel on Climate Change* ed T F Stocker, D Qin, G-K Plattner, M Tignor, S K Allen, J Boschung, A Nauels, Y Xia, V Bex and P M Midgley (Cambridge, United Kingdom: Cambridge University Press) 1535 doi:10.1017/CBO9781107415324
Jordà G 2014 Detection time for global and regional sea level trends and accelerations *J. Geophys. Res. Oceans* **119** 7164–74
Kessler W S and Taft B A 1987 Dynamic heights and zonal geostrophic transports in the central tropical Pacific during 1979-84 *J. Phys. Oceanogr.* **17** 97–122
Köhl A 2015 Evaluation of the GECCO2 ocean synthesis: transports of volume, heat and freshwater in the Atlantic *Q. J. R. Meteorol. Soc.* **141** 166–81
Landerer F W, Gleckler P J and Lee T 2014 Evaluation of CMIP5 dynamic sea surface height multi-model simulations against satellite observations , *Clim. Dyn.* **43** 1271–83
Levitus S *et al* 2012 World ocean heat content and thermosteric sea level change (0–2000 m), 1955–2010 *Geophys. Res. Lett.* **39** L10603
Lyu K, Zhang X, Church J A, Slangen A B A and Hu J 2014 Time of emergence for regional sea-level change *Nat. Clim. Change* **4** 1006–10
Mantua N J and Hare S R 2002 The pacific decadal oscillation *J. Oceanogr.* **58** 35–44
Mantua N J, Hare S R, Zhang Y, Wallace J M and Francis R C 1997 A Pacific interdecadal climate oscillation with impacts on salmon production *Bull. Am. Meteorol. Soc.* **78** 1069–79
Marcos M and Amores A 2014 Quantifying anthropogenic and natural contributions to thermosteric sea level rise *Geophys. Res. Lett.* **41** 2014GL059766
McGregor S, Holbrook N J and Power S B 2007 Interdecadal sea surface temperature variability in the equatorial pacific ocean: I. the role of off-equatorial wind stresses and oceanic rossby waves *J. Clim.* **20** 2643–58
Meinen C S and McPhaden M J 2000 Observations of warm water volume changes in the equatorial pacific and their relationship to El Niño and La Niña *J. Clim.* **13** 3551–9
Merrifield M A 2011 A shift in western tropical Pacific Sea level trends during the 1990s *J. Clim.* **24** 4126–38
Merrifield M A and Maltrud M E 2011 Regional sea level trends due to a Pacific trade wind intensification *Geophys. Res. Lett.* **38** L21605
Meyssignac B, Henry O, Palanisamy H and Cazenave A 2015 Advances in understanding regional sea level variations from 2D sea level reconstructions based on tide gauge records, in preparation
Meyssignac B, Becker M, Llovel W and Cazenave A 2012a An assessment of two-dimensional past sea level reconstructions over 1950–2009 based on tide-gauge data and different input sea level grids *Surv. Geophys.* **33** 945–72
Meyssignac B, Salas y Melia D, Becker M, Llovel W and Cazenave A 2012b Tropical Pacific spatial trend patterns in observed sea level: internal variability and/or anthropogenic signature? *Clim. Past* **8** 787–802
Milne G A, Gehrels W R, Hughes C W and Tamisiea M E 2009 Identifying the causes of sea-level change *Nat. Geosci.* **2** 471–8
Myhre G *et al* 2013 Anthropogenic and natural radiative forcing *Climate Change 2013: The Physical Science Basis. Contribution of Working Group I to the Fifth Assessment Report of the Intergovernmental Panel on Climate Change* ed T F Stocker, D Qin, G-K Plattner, M Tignor, S K Allen, J Boschung, A Nauels, Y Xia, V Bex and P M Midgley (Cambridge, United Kingdom: Cambridge University Press)
Palanisamy H, Cazenave A, Delcroix T and Meyssignac B 2015 Spatial trend patterns in the Pacific Ocean sea level during the altimetry era: the contribution of thermocline depth change and internal climate variability *Ocean Dyn.* **65** 341–56
Pierce D W 2001 Distinguishing coupled ocean-atmosphere interactions from background noise in the North Pacific *Prog. Oceanogr.* **49** 331–52
Power S, Delage F, Chung C, Kociuba G and Keay K 2013 Robust twenty-first-century projections of El Nino and related precipitation variability *Nature* **502** 541–5

Power S, Haylock M, Colman R and Wang X 2006 The predictability of interdecadal changes in ENSO activity and ENSO teleconnections *J. Clim.* **19** 4755–71

Ribes A, Azaïs J-M and Planton S 2010 A method for regional climate change detection using smooth temporal patterns *Clim. Dyn.* **35** 391–406

Richter K and Marzeion B 2014 Earliest local emergence of forced dynamic and steric sea-level trends in climate models *Environ. Res. Lett.* **9** 114009

Schneider N and Cornuelle B D 2005 The forcing of the pacific decadal oscillation* *J. Clim.* **18** 4355–73

Sen Gupta L C, Muir J N, Brown S J, Phipps P J, Durack D, Monselesan and Wijffels S E 2012 Climate drift in the CMIP3 models *J. Clim.* **25** 4621–40

Singh A, Delcroix T and Cravatte S 2011 Contrasting the flavors of El NINO-SOUTHERN OSCILLATION USINg sea surface salinity observations *J. Geophys. Res.* **116** 1–16

Skeie R B, Berntsen T K, Myhre G, Tanaka K, Kvalevåg M M and Hoyle C R 2011 Anthropogenic radiative forcing time series from pre-industrial times until 2010 *Atmos Chem Phys.* **11** 11827–57

Slangen A B A, Church J A, Zhang X and Monselesan D 2014 Detection and attribution of global mean thermosteric sea level change *Geophys. Res. Lett.* **41** 5951–9

Stammer D, Cazenave A, Ponte R M and Tamisiea M E 2013 Causes for contemporary regional sea level changes *Annu. Rev. Mar. Sci.* **5** 21–46

Taylor K E, Stouffer R J and Meehl G A 2012 An overview of CMIP5 and the experiment design *Bull. Am. Meteorol. Soc.* **93** 485–98

Thompson P R, Merrifield M A, Wells J R and Chang C M 2014 Wind-driven coastal sea level variability in the northeast pacific *J. Clim.* **27** 4733–51

Verdon D C and Franks S W 2006 Long-term behaviour of ENSO: Interactions with the PDO over the past 400 years inferred from paleoclimate records *Geophys. Res. Lett.* **33** L06712

Watson C S, White N J, Church J A, King M A, Burgette R J and Legresy B 2015 Unabated global mean sea-level rise over the satellite altimeter era *Nat. Clim. Change* **5** 565–8

Wittenberg A T 2009 Are historical records sufficient to constrain ENSO simulations? *Geophys. Res. Lett.* **36** L12702

Yasunaka S and Hanawa K 2003 Regime shifts in the northern hemisphere SST field: revisited in relation to tropical variations *J. Meteorol. Soc. Jpn. Ser II* **81** 415–24

Yeh S-W, Kug J-S, Dewitte B, Kwon M-H, Kirtman B P and Jin F-F 2009 El Niño in a changing climate *Nature* **461** 511–4

Yin J 2012 Century to multi-century sea level rise projections from CMIP5 models *Geophys. Res. Lett.* **39** 17709

Yin J, Griffies S M and Stouffer R J 2010 Spatial variability of sea level rise in twenty-first century projections *J. Clim.* **23** 4585–607

Zhang X and Church J A 2012 Sea level trends, interannual and decadal variability in the Pacific Ocean *Geophys. Res. Lett.* **39**

Zhang Y, Wallace J M and Battisti D S 1997 ENSO-like interdecadal variability: 1900–93 *J. Clim.* **10** 1004–20